

MODELING THE SELECTIVITY OF DIELS ALDER REACTIONS IN VARIOUS
MEDIA

by

Gamze Bahadır

B.S., Chemistry, Boğaziçi University, 2013

Submitted to the Institute for Graduate Studies in
Science and Engineering in partial fulfillment of
the requirements for the degree of
Master of Science

Graduate Program in Department of Chemistry
Boğaziçi University

2016

To all immigrant children.

ACKNOWLEDGEMENTS

Firstly, I would like to express my deepest gratitude to my thesis advisor Prof. Viktorya Aviyente, to whom I am very thankful for her guidance, support and patience during my thesis work. It was a very great opportunity for me to be her student and be able to learn from her scientific excellence. I would like also to express special thanks to Prof. Ilknur Dogan and Associate Prof. Aylin Konuklar as the members of my committee. Furthermore, I would like to thank to Assist. Prof. Saron Catak, for her valuable comments during my research progress and to Sesil Agopcan Cinar for all her motivation and patience to all my questions. I would like to share all my thankful feelings to my colleagues from the Computational Chemistry Group, Büsra Dereli, Tugçe Erbay, Pinar Haslak, Tugba Furuncuoglu, Özlem Karahan, Gülsah Çifci, Ilke Ugur, Burcu Dedeoglu, Deniz Akgül, Berkehan Kura, Kumru Dikmenli, Taylan Akdogan, Semiha Bali and Birce Kahraman. I am very privileged to have had the opportunity to work with all of them.

I would like to thank to all members of Bogaziçi Chemistry Department. I was very lucky to be able to take courses from the wise professors and share the welcoming atmosphere of department.

I am also very thankful to Prof. Hendrik Zipse and Dr. Johnny Hioe from Ludwig Maximilian University of Munich for all their support and fruitful time of my Erasmus period.

I would like to thank also to my friends, Gül Öncü, Önder Abbatai, Derya Karagöz, Metin Uyar, Mustafa Altinoluk, Murat Ari, Elif Kurnaz, Ece Çiftçi, Özlem Büyükgümüs, Sinem Palantöken, Duygu Baykal, Nigar Asgarova, Emre Çelebi, Basak Helvacı and Erhan Özaçar for all their endless love and all happy moments they created for me.

Moreover, I would like to thank to Mr. Erol Margunato and Mr. Cem Margunato, for their support and the invaluable chances at work as lifelong experiences and to my colleagues, Seda Yilmaz, Furkan Övündür, Selin Aydın, Sema Orhan, Sebahat Abakbigan and Sema Yilmaz, Cengiz Erdogan and Nilgün Yaldiz.

I would like to express also my great appreciation to my teachers, Aylin Vartanyan, Meltem Gürle, Nilüfer Andiç and Esmâ Bayir. They are very important roles for me to broaden my vision.

Last but not least, I want to thank to Safak Söylemez for his sincere encouragement with all his warm accompany and to my family for all their contributions to my life to mature and for their love and patience throughout my life.

ABSTRACT

MODELING THE SELECTIVITY OF DIELS ALDER REACTIONS IN VARIOUS MEDIA

The goal of this research is to model and understand the Diels-Alder and 1,3-dipolar cyclo addition type of reactions in divergent media via two main reactions. In the first part of this dissertation the *exo/endo* selectivity for the heterocyclic Diels Alders reaction of the diene, 5-benzylidene-2-arylimino-3-aryl-thiazolidine-4-thione and the dienophile alpha-pinene has been modeled. The mechanism of the reaction has been simulated by using the quantum mechanical method via the B3LYP/6-31+G(d) methodology. The stereoselectivity is investigated for Diels Alder's reaction of a heterocyclic addition reaction including minus alpha-pinene as a dienophile and a diene. The mechanism of the reaction is modeled and the activation energy barriers are calculated. The activation energy barriers are relatively high according to the results of the computational calculations and the reason of not being able to run the experimental reactions is clarified. The second part of the dissertation aims to investigate the increase of *endo* selectivity of Diels Alder reactions in ionic liquids. Three main Diels Alder's reactions of cyclopentadiene as a diene and three derivatives of methyl methacrylate as dienophile are simulated in ethanol. The B3LYP/6-31+G(d) level of theory is utilized to model the respective reactions. These reactions have been modeled and the proportion of the *endo/exo* product ratio for the formation of the products has been calculated. The ratio derived from these calculations is consistent with the experimental results taken from the literature. The ionic liquid effect to the increase of the *endo* selectivity is investigated for three reactions. 1-ethyl-3-methylimidazolium chloride is utilized as the ionic liquid. The increase in the formation of the *endo* product is obtained from the calculations.

ÖZET

ÇEŞİTLİ KİMYASAL ORTAMLARDA DIELS ALDER TEPKİMELERİNİN SEÇİCİLİĞİNİN MODELLEMESİ

Bu araştırmanın amacı, Diels Alder ve 1,3 dipolar siklo katılma tipinde iki ana tepkimenin çeşitli kimyasal ortamlarda anlaşılması ve modellenmesidir. Bu tezin ilk bölümündedien 5-benziliden-2-arilimino-3-aril-tiazolidin-4-tiyon vedienofil alfa-pinenin heterosiklik Diels Alder tepkimesi için *ekzo* / *endo* seçiciliği modellenmiştir. Tepkimenin mekanizması B3LYP/6-31+G(d) yöntemiyle kuantum mekaniksel yöntemi kullanılarak simüle edilmiştir. Stereo seçicilik dienofil olarak eksi alfa-pinenve 5-benziliden-2-arilimino-3-aril-tiazolidin-4-tiyon molekülü dien olmak üzere bir heterosiklik katılma tepkimesi için araştırılmıştır. Tepkimenin mekanizması modellenmiş ve aktivasyon enerjileri hesaplanmıştır. Hesaplanan aktivasyon enerjilerinin göreceli olarak yüksek olması deneysel tepkimelerinden yürütülemediğine açıklık getirmiştir. Tezin ikinci bölümünde iyonik sıvı ortamında *endo* seçiciliğinin *exo* seçiciliğe oranla artışın araştırılması amaçlanmıştır. Dien olarak siklopentadienin ve diofil olarak metilmetakrilatın türevleri üç ana Diels Alder tepkimeleri etanolde simüle edilmiştir. B3LYP/6-31+G(d) yöntemi ilgili tepkimeleri modellemek için kullanılmaktadır. Bu tepkimeler modellenmiş ve oluşmakta olan *endo* / *exo* ürünün oranı hesaplanmıştır. Hesaplardan gelen bu oran literatürden alınan deneysel sonuçlarla uyusmaktadır. Exo seçiciliğe karşın *endo* seçiciliğinin artışındaki iyonik sıvı etkisi üç ana reaksiyo nüzlerinde incelenmiştir. İyonik sıvı olarak 1-etil-3-metilimidazolium klorür kullanılmıştır. İyonik sıvı etkisiyle *endo* ürün oluşumunun arttığı hesaplarda bulunmuştur.

TABLE OF CONTENTS

ACKNOWLEDGEMENTS	iv
ABSTRACT	vi
ÖZET	vii
LIST OF FIGURES	ix
LIST OF TABLES	xii
LIST OF SYMBOLS	xiii
LIST OF ACRONYMS/ABBREVIATIONS	xiv
1. INTRODUCTION	1
1.1. General	1
2. METHODOLOGY	10
2.1. Density Functional Theory	10
2.2. Continuum Solvation Models	14
3. AIM OF THE STUDY	18
4. RESULTS AND DISCUSSION	19
4.1. Modeling the Diels Alder Reaction of thiones with α -pinene	19
4.2. Modeling the Diels Alder Reactions of Cyclopentadiene with Methacrylate Derivatives	27
4.2.1. Modeling the Diels Alder Reactions of Cyclopentadiene with Methacrylate Derivatives in the Absence of Ionic Liquids	27
4.2.2. Modeling the Diels Alder Reactions of Cyclopentadiene with Methacrylate Derivatives in the Presence of Ionic Liquids	32
5. CONCLUSION	37
6. FUTURE WORK	38
REFERENCES	39

LIST OF FIGURES

Figure 1.1.	An Illustration of the Diels Alder's Reaction [1].	1
Figure 1.2.	An Example of Addition of a Cyclic Diene.	2
Figure 1.3.	Frontier Molecular Orbital Interaction of Diels-Alder Reaction of Butadiene and Ethylene [2].	2
Figure 1.4.	An Example of <i>endo</i> and <i>exo</i> Transition States Taken from the Study of Andrushko <i>et al.</i> , [4].	3
Figure 1.5.	An Example of Diels Alder Cycloaddition.	4
Figure 1.6.	An Example of <i>exo</i> and <i>endo</i> Product.	4
Figure 1.7.	A Representation of the 4 Possible Structures derived from the Combination of a Cyclo diene with Dienophile.	5
Figure 1.8.	An Example of <i>exo</i> -selectivity in the Transition States [5].	5
Figure 1.9.	The Reactions of Methacrylate Derivatives with Cyclopentadiene taken from the Article of Kumar <i>et al.</i> , [15].	9
Figure 4.1.	Representation of the Mechanism of the Reaction of (+) - α - Pinene with 5 - Benzylidene - 2 - Arylimino - 3 - Aryl - Thiazolidine - 4 - Thione.	20
Figure 4.2.	The Structure of the Diene, 5 - ((Z) - Benzylidene) - 3 - Phenyl - 2 - (Phenylimino) Thiazolidine - 4 - Thione.	21

Figure 4.3.	The Structures of the two Stereoisomers of the Dienophile, Alpha Pinene with B3LYP/6-31+G(d).	21
Figure 4.4.	Diels Alder Reaction of 5 - ((Z) - Benzylidene) - 3 - Phenyl - 2 - (Phenylimino) Thiazolidine - 4 - Thione with (-) α - Pinene. . . .	22
Figure 4.5.	Products with S3C10 Connectivity Geometry. Relative Gibbs Free Energies are Given Below the Structures, in kcal/mol at 298.150 K and 1 atm.	23
Figure 4.6.	Products with S3C2 Connectivity Geometry. Relative Gibbs Free Energies are Given below the Structures, in kcal/mol at 298.150K and 1 atm.	24
Figure 4.7.	Transition States with S3C10 Connectivity Geometry. Relative Gibbs free Energies are given Below the Structures, in kcal/mol at 298.150 K and 1 atm.	25
Figure 4.8.	Transition States with S3C2 Connectivity Geometry. Relative Gibbs free Energies are Given Below the Structures, in kcal/mol at 298.150 K and 1 atm.	25
Figure 4.9.	The Positions of the Stereo Centers of the Molecules.	28
Figure 4.10.	The Positions of the Stereo Centers of the MoleculesRelative Gibbs Freeenergy of the Conformersofthe Dienophile Modeled in Ethanol. . . .	30
Figure 4.11.	Activation Energies of the Transition State Structures Modeled in Ethanol.	31
Figure 4.12.	Relative Gibbs Free Energies of Products Modeled in Ethanol. . . .	31

Figure 4.13. Numbering Used in Methyl Metacrylate Derivatives.	32
Figure 4.14. 1-Ethyl-3-Methylimidazolium Cation with its NPA Charges on the Hydrogen Atoms.	34
Figure 4.15. Reactants with Ionic Liquid Modeled with B3LYP/6-31+G(d) in Ethanol.	34
Figure 4.16. Transition State Structures Modeled with B3LYP/6-31+G(d) in Ethanol.	35
Figure 4.17. Product Structures Modeled with B3LYP/6-31+G(d) in Ethanol.	35

LIST OF TABLES

Table 4.1.	Thermodynamic Results of the Products Calculated with B3 LYP / 6 - 31 + G(d) at 298.150 K and 1 Atmin Gaseous Phase.	24
Table 4.2.	Kinetic Data of the Transition State forms Calculated at 298.150 K and 1 atm in Gas.	26
Table 4.3.	The Thermodynamic and Kinetic Results of the Molecules via B3 LYP / 6 - 31 + G(d) at 298.150K and 1 atm. Gibbs free Energies are given in (kcal/mol).	28
Table 4.4.	The <i>exo-endo</i> Ratios Calculated in the Absence of Ionic Liquid in Ethanol.	29
Table 4.5.	NPA charges on the reactant with B3LYP/6-31+G(d) in ethanol.	32
Table 4.6.	The Thermodynamic and Kinetic Results of the Molecules at 298.150 K and 1 atm. Gibbs Free Energies are given in kcal/mol.	33
Table 4.7.	The <i>exo-endo</i> Ratios Calculated in the Presence of Ionic Liquid in Ethanol.	34

LIST OF SYMBOLS

$B3LYP$	Becke-3-parameter Lee-Yang-Parr functional
$B88$	Becke 88 Exchange Functional
E_x^{exact}	Exact exchange energy
$E_c[\rho]$	Correlation energy
$E_x[\rho]$	Exchange energy
$E_{\sigma\sigma^*}$	Non-covalent contributions to the energy
HF	Hartree-Fock theory
$J[\rho]$	Coulomb energy
QM	Quantum Mechanics
$T_s[\rho]$	Kinetic Energy
V_{KS}	Kohn-Sham potential
$v(r)$	External potential
ΔE^\ddagger	Electronic activation energy
ΔG^\ddagger	Gibbs free energy of activation
ΔE_x^{B88}	Becke's gradient correction
ΔE_0	Relative electronic energy at 0 K
ΔE_{0+ZPE}	Sum of the change in electronic energy, zero point energy at 0K
ΔH_{rxn}	Enthalpy of reaction as electronic energy
$\rho(r)$	Electron density
ψ_i	Kohn-Sham orbitals

LIST OF ACRONYMS/ABBREVIATIONS

DA	Diels Alder
DFT	Density Functional Energy
IEDDA	Inverse Electron Demand Diels-Alder
LDA	Local Density Approximation

1. INTRODUCTION

1.1. General

Diels Alder (DA) reactions are one of the icebreaking points in Organic Chemistry. Otto Paul Hermann Diels and Kurt Alder were awarded with the Nobel Prize in Chemistry in 1950. Diels Alder's reaction is the most powerful synthetic method for unsaturated six-membered rings with its simplicity of operation. These reactions are the cycloaddition of a conjugated diene and a dienophile. The driving force of the reaction is the formation of new σ -bonds, which are energetically more stable than the π -bonds on the respective molecules. These reactions are [4+2] cycloaddition reactions and are widely utilized to synthesize a six membered ring with up to four stereogenic centers possessing a regio-selectivity and stereo-control as it is indicated in Figure 1.1 [1].

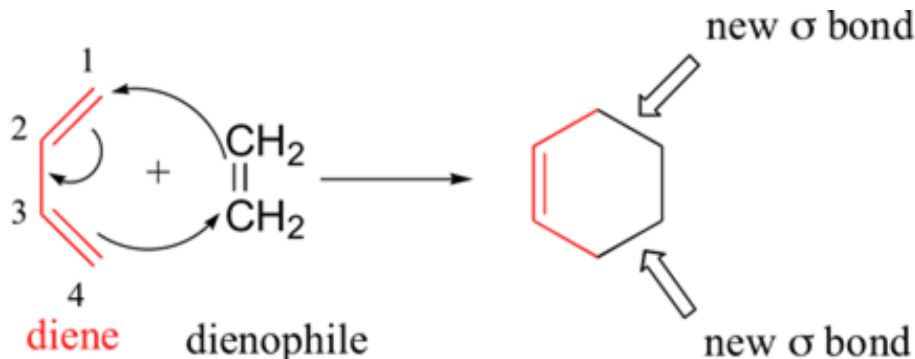


Figure 1.1. An Illustration of the Diels Alder's Reaction [1].

The same mechanism as above is valid for the cyclic molecules as indicated in Figure 1.2.

The tendency of Diels-Alder Reactions to be electronically favorable to form proper transition states is dependent on orbital symmetry [1]. Kenichi Fukui's molecular orbital model offer a flow of electrons from the highest occupied molecular orbital (HOMO) of one reactant or participating bond to the lowest unoccupied molecular

orbital (LUMO) of another reactant or bond.



Figure 1.2. An Example of Addition of a Cyclic Diene.

A flow of electrons from the highest occupied molecular orbital (HOMO) to the lowest unoccupied molecular orbital (LUMO) of another reactant or bond is the main assumption of the frontier-orbital model for the respective mechanism of Diels-Alder reactions as it is indicated in the Figure 1.3.

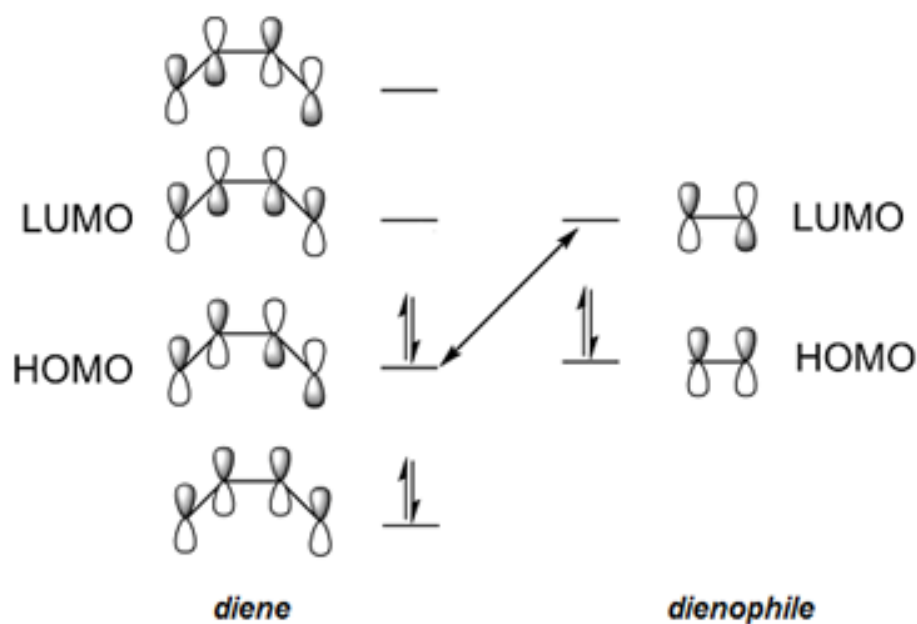


Figure 1.3. Frontier Molecular Orbital Interaction of Diels-Alder Reaction of Butadiene and Ethylene [2].

According to the flow of the electron and the synchronicity in the interaction to form a transition state there are different types of Diels-Alder reactions. The syn-

chronous concerted reaction is the one where the two bonds of the cycloadduct are formed at the same time; while the stepwise formation of the two bonds is asynchronous [3]. The normal DA reactions are driven by the attack of the diene, as being the electron rich group to the dienophile. However, there are some mechanisms where the diene and the dienophile change their roles and the tendency of the electrons is in an inverse direction. These types of the reactions are called the inverse electron demand Diels-Alder (IEDDA) reactions where heterocyclic rings are involved and take place at high temperature condition. The inverse electron flow has the path of $\text{LUMO}_{\text{diene}} \rightarrow \text{HOMO}_{\text{dienophile}}$.

In order to have a deeper understanding of the mechanism of cycloaddition reaction, an example of a substituted dienophile having two possible stereo chemical orientations with respect to its diene is considered. The transition state of the respective reaction is named as *endo* or *exo* according to the position of the substituent on p orbitals of the diene. If the substituent is oriented away from the p system of the diene, this transition state is an *exo* type; if the substituent on the dienophile is oriented toward the p orbitals of the diene, the transition is called as *endo* transition state as it is indicated in the Figure 1.4 [4].

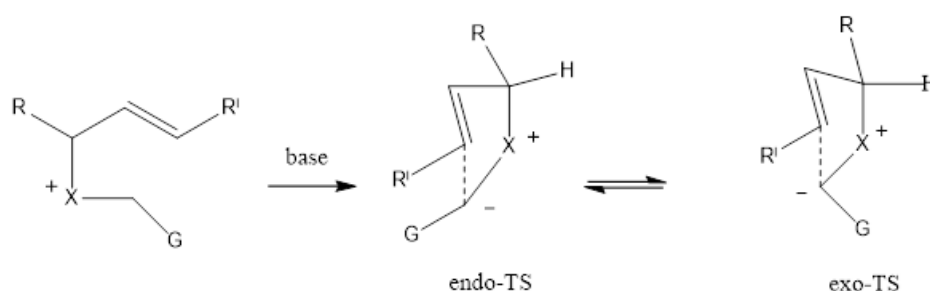


Figure 1.4. An Example of *endo* and *exo* Transition States Taken from the Study of Andrushko *et al.*, [4].

The different orientation of the bond formation leads to the *exo/endo* types of product. If the bulk group is inside the concave group; it is named as *endo*; if it is outside of the concave group; it is named as *exo*. Figure 1.5 indicates an example of how attacks effect the orientation in the product and can lead to be *exo* and *endo*

products.

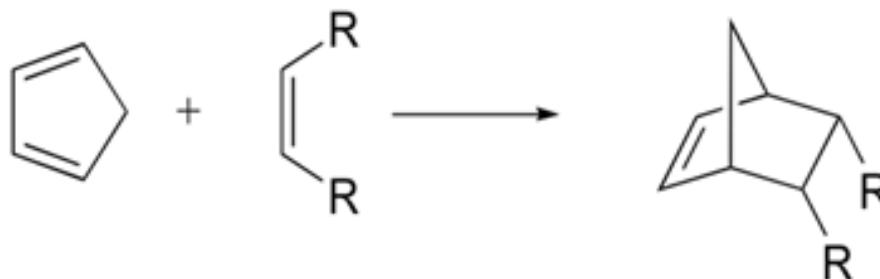


Figure 1.5. An Example of Diels Alder Cycloaddition.

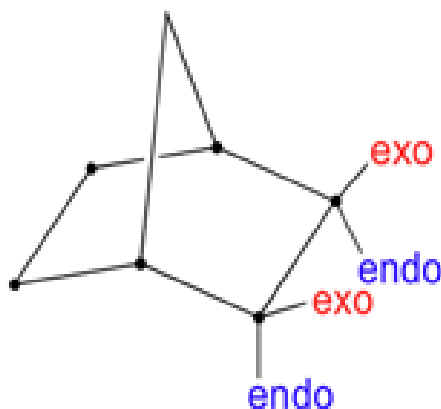


Figure 1.6. An Example of *exo* and *endo* Product.

Endo is inside the concave side of the six-membered ring. The possible number of transition states may increase with more substituted cycloaddienes. These different combinations will lead to different types of products.

The possible paths of the combination of norbornene with a cycloaddiene are indicated in Figure 1.7. The importance of the selectivity among all these reactions comes from the different stereogenic centers. The divergent stereochemistry is very important in a lot of application in the industry. Therefore, the *endo* or *exo* selectivity is investigated targeting to have results of one desired product by changing either the geometry of the reactants or modifying the media of the respective reactions held.

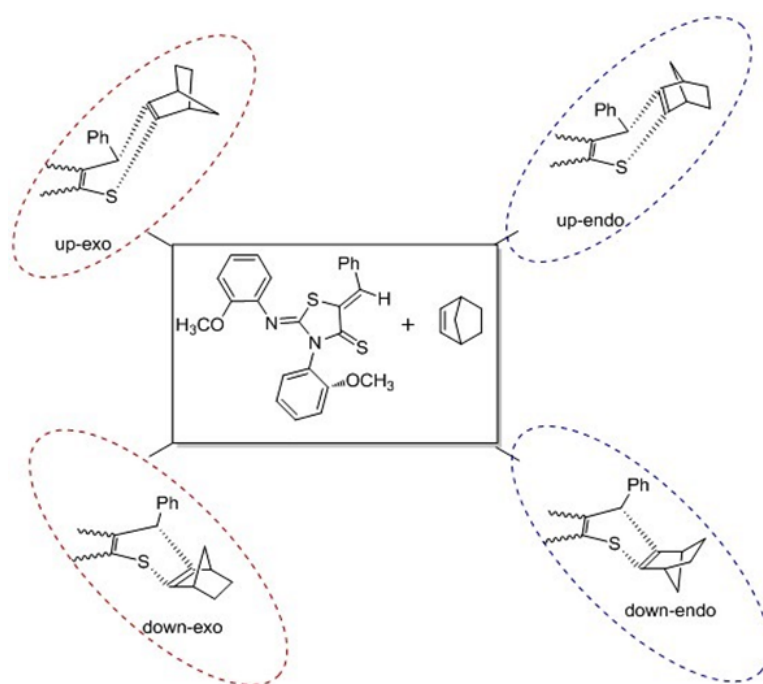


Figure 1.7. A Representation of the 4 Possible Structures derived from the Combination of a Cyclodiene with Dienophile.

An example of exo selectivity among the endo, one of transition states with thermodynamic indication by Houket al. is indicated in the Figure 1.8 [5].

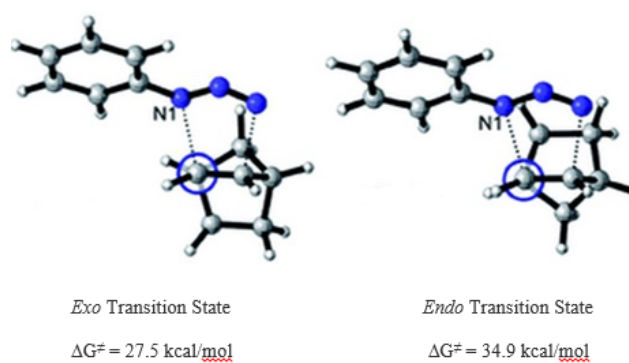


Figure 1.8. An Example of exo-selectivity in the Transition States [5].

Another inspiring research achieved on the selectivity of Diels Alder's reactions is the computational study named as "Origins of exo-Stereoselectivity of Norbornene in Hetero Diels-Alder Reactions" by Aviyente *et al.*, [6], where the mechanism and the

exo or endo selectivity of the reaction is investigated and the findings are compared with the experimental results. Norbornene is adapted as the case study for the models of the reactions since exo selectivity of norbornene and its high reactivity in Diels-Alder reaction is a matter of interest in organic chemistry [12]. The experimental part of this study is performed by Dogan *et al.*, with atropisomeric 5-benzylidene-2-arylimino-3-aryl-thiazolidine-4-thiones being utilized as heterodienes in the inverse electron-demand hetero Diels-Alder cycloadditions with norbornene with the role of a dienophile at 25 °C [13]. The findings of this study gave 100% exo-selectivity as determined by NMR experiments [14]. The experiments are investigated also with quantum chemical computational tools and the result of the kinetic and thermodynamic data resulted from the investigations of Aviyente *et al.*, is found to be consistent with the experimental results [6].

Diels Alder's reactions are utilized for the production of different kinds of products such as pharmaceutical drugs, agrochemical compounds, flavors and fragrances in industries. Especially, the cycloaddition of this reaction is very popular with regard of the selectivity of *endo* or *exo* type of products. The functions, chemical and mechanical properties of *exo* products are different than *endo* products. Therefore, the progress of the reaction is shifted to the desired path. Solvation catalyst additions are some methods used to increase the rate of the targeted orientation of the end product. Ionic liquids are used to enhance the selectivity; because they are environmental friendly, have ionic and thermal stability. Moreover, they can act as catalysts and can be reused after another reaction. The chemical stability, high internal pressure, hydrogen bonding, Lewis acidity and solvent polarity are very important properties that make the ionic liquids function as it is narrated above [7]. There are some kinds of ionic liquids utilized to benefit from the divergent results. For example, ionic liquids have an important impact on the kinetics and the yield according to Sahu *et al.*, work. Sahu *et al* have utilized ionic liquids to enhance the endo yield of the products formed [8].

There are many types of ionic liquids of both experimental and in silico studies. The chemical properties of the ionic liquid is having two parts of cation and anion, being able to give electrical stability to the solution. Being the melted version of the salt with

an organic group, the ionic liquids have good compatibility with the organic reactions [9]. Another application of the ionic liquids is to be mediated of a Diels Alder's reaction catalyst. Three different types of ionic liquid like 1-butyl-3-methylimidazolium chloride ([BMIM] Cl), 1-butyl-3-methylimidazolium hexa fluorophosphates ([BMIM][PF6]) and 1-butyl-3-methylimidazolium bis(trifluoromethanesulfonyl)imide ([BMIM][NTF2]) were tested as a reaction medium for MacMillan's imidazolidinone catalyst to catalyzed our model Diels-Alder reaction between cyclo hexadiene and acrolein [9].

1-Butyl-3-methylimidazolium chloride [BMIM]Cl was synthesized by Dharaskar via nucleophilic substitution reaction of 1-methylimidazole and 1-chlorobutane. The molecular structure of [BMIM]Cl was confirmed by FTIR, ¹H-NMR, and ¹³C-NMR. The thermal properties, conductivity, solubility, water content and viscosity analysis of [BMIM]Cl were found experimentally. The effects of reaction time, reaction temperature, sulfur compounds, and recycling of the respective ionic liquid without regeneration on dibenzothiophene removal of liquid fuel were presented. The results of this work offered significant insights in the perceptive use of imidazoled ionic liquids as energy-efficient green material for extractive deep desulfurization of liquid fuels because they can be reused without regeneration with considerable extraction efficiency [10].

1-butyl-3-methylimidazolium hexafluorophosphate [BMIM-PF6] is another member of the ionic liquid family. 1-butyl-3-methylimidazolium hexafluorophosphate being a viscous, colorless, hydrophobic is a non-water-soluble ionic liquid with a melting point of -8 °C [11]. Together with 1-butyl-3-methylimidazolium tetrafluoroborate [BMIM-BF4], is one of the most widely utilized ionic liquids for divergent targets. It slowly decomposes in the presence of water [12]. BMIM-PF6 is both commercially available or it can be produced. The synthesis can be achieved by alkylating 1-methylimidazole with 1-chlorobutane. A metathesis reaction with potassium hexafluorophosphate gives the desired compound [13].

Another two important examples of ionic liquids involved in the Sahu et al's study are 1 ethyl 3 methylimidazolium chloride [EMICl] and 1 ethyl 3 methylimidazolium

heptachlorodialuminate [EMIA₂Cl₇]. 1-ethyl-3-methylimidazolium chloride is an ionic liquid which can be utilized in cellulose processing and as a catalyst. The ionic liquid possesses two parts of cation of 1-ethyl-3-methylimidazolium and anion of chloride. The cation consists of a five-membered ring with two nitrogen and three carbon atoms, i.e. a derivative of imidazole, with ethyl and methyl groups substituted at the two nitrogen atoms. Its melting point is 77-79 °C [14].

1-ethyl-3-methyl-imidazolium heptachlorodialuminate is utilized as both solvent and as catalyst due to the aluminate group functionalizing as Lewis Acid catalyst. It consists two parts, where the cation is 1-ethyl-3-methylimidazolium and anion of heptachlorodialuminate.

The cycloaddition of cyclopentadiene with methyl methacrylate is a very attractive example of Diels Alder's reactions leading to *endo:exo* products. The *endo:exo* ratio for the Diels Alder's reaction of cyclopentadiene with methyl methacrylate is investigated with the inspiration of the experimental work of Anil Kumar and Sanjay S. Pawar.

The following three main reactions are modeled and the results of the *endo:exo* selectivity are compared with the experimental results [15]. The reactants of methacrylate derivatives and cyclopentadiene, their products and transition states are modeled in ethanol in an implicit solvation. Scheme 1.1 indicates the three main reactions taken from Kumar *et al.*'s work [15].

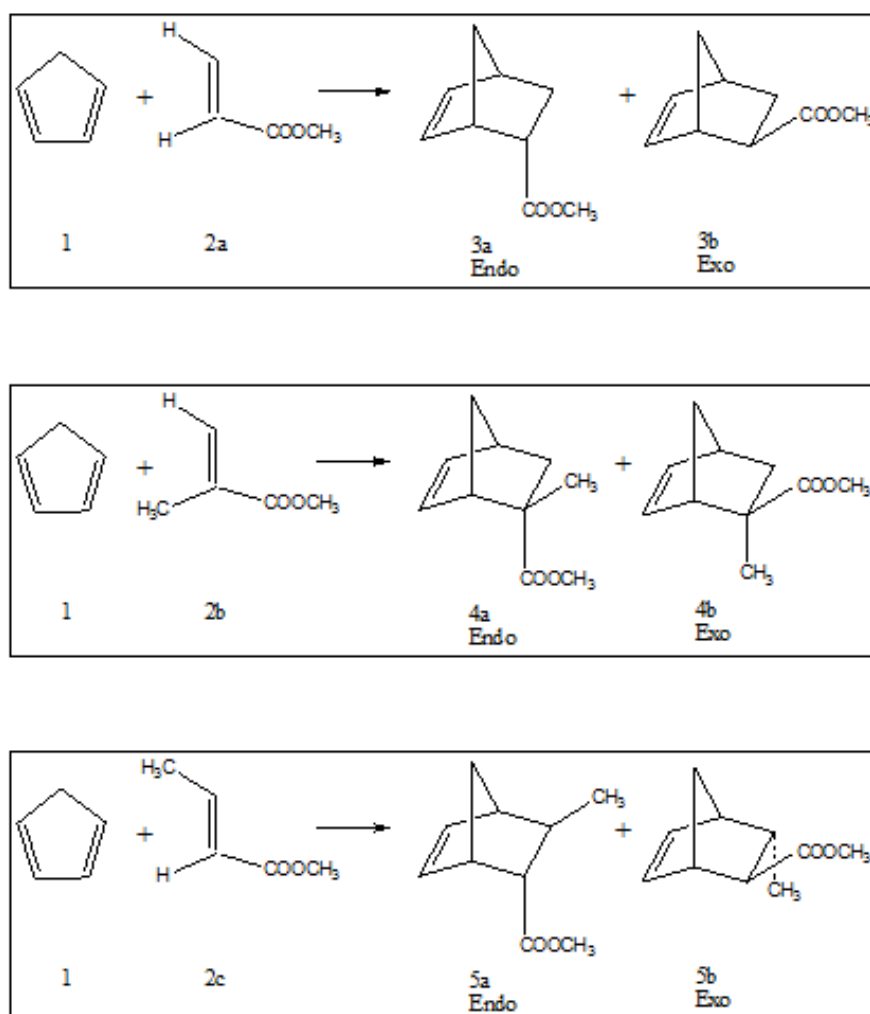


Figure 1.9. The Reactions of Methacrylate Derivatives with Cyclopentadiene taken from the Article of Kumar *et al.*, [15].

2. METHODOLOGY

2.1. Density Functional Theory

Density Functional Theory (DFT) is rooted from Kohn-Hohenberg theorems that are suggested in 1964 [16]. Being the quantum mechanical approach to the electronic nature of particles, the theorems offer that the ground-state properties of a molecular system are functions of the charge density parameter [17].

The former theorem explains the external potential $V_{ext}(\mathbf{r})$ dependent on the electron density $\rho(\mathbf{r})$ [18]. The latter one states the variation principle. As a result, the electron density can be computed variationally and the position of nuclei, energy, wave function and other related parameters can be calculated [19].

The electron density is defined as follows:

$$\rho(x) = N \int \cdots \int |\Psi(x_1, x_2, \cdots, x_n)|^2 dx_1 dx_2 \cdots dx_n \quad (2.1)$$

where x stands for both spin and spatial coordinates of electrons.

The electronic energy can be defined as a functional of the electron density:

$$E[\rho] = \int v(r) \rho(r) dr + T[\rho] + V_{ee}[\rho] \quad (2.2)$$

where $T[\rho]$ is the kinetic energy of the interacting electrons and $V_{ee}[\rho]$ is the interelectronic interaction energy. The electronic energy may be rewritten as

$$E[\rho] = \int v(r) \rho(r) dr + T_s[\rho] + J[\rho] + E_{xc}[\rho] \quad (2.3)$$

with $J[\rho]$ being the coulomb energy, $T_s[\rho]$ being the kinetic energy of the non-interacting electrons and $E_{xc}[\rho]$ being the exchange-correlation energy functional. The exchange-

correlation functional is expressed as the sum of an exchange functional $E_x[\rho]$ and a correlation functional $E_c[\rho]$, although it contains also a kinetic energy term arising from the kinetic energy difference between the interacting and non-interacting electron systems. The kinetic energy term, being the measure of the freedom, and exchange-correlation energy, describing the change of opposite spin electrons (defining extra freedom to an electron), are the favorable energy contributions. The Coulomb energy term describes the unfavorable electron-electron repulsion energy and therefore disfavors the total electronic energy [20].

In Kohn-Sham density functional theory, a reference system of independent non-interacting electrons in a common, one-body potential V_{KS} yielding the same density as the real fully-interacting system is considered. More specifically, a set of independent reference orbitals ψ_i satisfying the following independent particle Schrödinger equation are imagined.

$$\left[-\frac{1}{2}\nabla^2 + V_{KS} \right] \psi_i = \varepsilon_i \psi_i \quad (2.4)$$

with the one-body potential VKS defined as

$$V_{KS} = v(r) + \frac{\partial J[\rho]}{\partial \rho(r)} + \frac{\partial E_{xc}[\rho]}{\partial \rho(r)} \quad (2.5)$$

$$V_{KS} = v(r) + \int \frac{\rho(r')}{|r-r'|} dr' + v_{xc}(r) \quad (2.6)$$

Where $v_{xc}(r)$ is the exchange-correlation potential. The independent orbitals ψ_i are known as Kohn-Sham orbitals and give the exact density by

$$\rho(r) = \sum_i N |\psi_i|^2 \quad (2.7)$$

if the exact form of the exchange-correlation functional is known. However, the exact form of this functional is not known and approximate forms are developed starting

with the local density approximation (LDA). This approximation gives the energy of a uniform electron gas, i.e. a large number of electrons uniformly spread out in a cube accompanied with a uniform distribution of the positive charge to make the system neutral. The energy expression is

$$E[\rho] = T_s[\rho] + \int \rho(r) v(r) dr + J[\rho] + E_{xc}[\rho] + E_b \quad (2.8)$$

where E_b is the electrostatic energy of the positive background. Since the positive charge density is the negative of the electron density due to uniform distribution of particles, the energy expression is reduced to

$$E[\rho] = T_s[\rho] + E_{xc}[\rho] \quad (2.9)$$

$$E[\rho] = T_s[\rho] + E_x[\rho] + E_c[\rho] \quad (2.10)$$

The kinetic energy functional can be written as

$$T_s[\rho] = C_F \int \rho(r)^{5/3} dr \quad (2.11)$$

where C_F is a constant equal to 2.8712. The exchange functional is given by

$$E_x[\rho] = -C_x \int \rho(r)^{4/3} dr \quad (2.12)$$

with C_x being a constant equal to 0.7386. The correlation energy, $E_c[\rho]$, for a homogeneous electron gas comes from the parameterization of the results of a set of quantum Monte Carlo calculations.

The LDA method underestimates the exchange energy by about 10 per cent and does not have the correct asymptotic behavior. The exact asymptotic behavior of the

exchange energy density of any finite many-electron system is given by

$$\lim_{x \rightarrow \infty} U_x^\sigma = -\frac{1}{r} \quad (2.13)$$

U_x^σ Being related to $E_x[\rho]$ by

$$E_x[\rho] = \frac{1}{2} \sum_{\sigma} \int \rho_{\sigma} U_x^{\sigma} dr \quad (2.14)$$

A gradient-corrected functional is proposed by Becke

$$E_x = E_x^{LDA} - \beta \sum_{\sigma} \int \rho_{\sigma}^{4/3} \frac{x_{\sigma}^2}{1 + 6\beta x_{\sigma} \sinh^{-1} x_{\sigma}} dr \quad (2.15)$$

Where σ denotes the electron spin, $x_{\sigma} = \frac{|\nabla \rho_{\sigma}|}{\rho_{\sigma}^{4/3}}$ and β is an empirical constant ($\beta=0.0042$).

This functional is known as Becke88 (B88) functional [21].

The adiabatic connection formula connects the non-interacting Kohn-Sham reference system ($\lambda=0$) to the fully-interacting real system ($\lambda=1$) and is given by

$$E_{xc} = \int_0^1 U_{xc}^{\lambda} d\lambda \quad (2.16)$$

where λ is the interelectronic coupling-strength parameter and U_{xc}^{λ} is the potential energy of exchange-correlation at intermediate coupling strength. The adiabatic connection formula can be approximated by

$$E_{xc} = \frac{1}{2} E_x^{exact} + \frac{1}{2} U_{xc}^{LDA} \quad (2.17)$$

Since $U_{xc}^0 = E_x^{exact}$, the exact exchange energy of the Slater determinant of the Kohn-Sham orbitals, and $U_{xc}^1 = U_{xc}^{LDA}$ [22].

The closed shell Lee-Yang-Parr (LYP) correlation functional [22] is given by

$$E_c = -a \int \frac{1}{1+d\rho^{-1/3}} \left\{ \rho + b\rho^{-2/3} \left[C_F \rho^{5/3} - 2t_w + \left(\frac{1}{9}t_w + \frac{1}{18}\nabla^2\rho \right) \right] e^{-c\rho^{-1/3}} \right\} dr \quad (2.18)$$

where

$$t_w = \frac{1}{8} \frac{|\nabla\rho(r)|^2}{\rho(r)} - \frac{1}{8} \nabla^2\rho \quad (2.19)$$

The mixing of LDA, B88, E_x^{exact} and the gradient-corrected correlation functionals to give the hybrid functional [21] involves three parameters.

$$E_{xc} = E_{xc}^{LDA} + a_0 \left(E_x^{exact} - E_x^{LDA} \right) + a_x \Delta E_x^{B88} + a_c \Delta E_c^{non-local} \quad (2.20)$$

where ΔE_x^{B88} is the Becke's gradient correction to the exchange functional, in the B3LYP functional, the gradient-correction ($\Delta E_c^{non-local}$) to the correlation functional is included in LYP. However, LYP contains also a local correlation term which must be subtracted to yield the correction term only.

$$\Delta E_c^{non-local} = E_c^{LYP} - E_c^{VWN} \quad (2.21)$$

where E_c^{VWN} is the Vosko-Wilk-Nusair correlation functional, a parameterized form of the LDA correlation energy based on Monte Carlo calculations. The empirical coefficients are $a_0=0.20$, $a_x=0.72$ and $a_c=0.81$ [24].

2.2. Continuum Solvation Models

The most efficient way to include condensed-phase effects into quantum mechanical calculations is the continuum solvation models [25]. The advantage of these models is that they decrease the number of the degrees of freedom of the system by describ-

ing them in a continuous way, usually by means of a distribution function [26-27]. In continuum solvation models, the solvent is represented with a polarizable medium characterized by its static dielectric constant ϵ and the solute is embedded in a cavity surrounded by this dielectric medium. The total solvation free energy is defined as

$$\Delta G_{solvation} = \Delta G_{cavity} + \Delta G_{dispersion} + \Delta G_{electrostatic} + \Delta G_{repulsion} \quad (2.22)$$

where ΔG_{cavity} is the energetic cost of placing the solute in the medium. Dispersion interactions between solvent and solute are expressed as $\Delta G_{d,dispersion}$ which add stabilization to solvation free energy. $\Delta G_{electrostatic}$ is the electrostatic component of the solute-solvent interaction energy. $\Delta G_{repulsion}$ is the exchange solute-solvent interactions not included in the cavitation energy.

The central problem of continuum solvent models is the electrostatic problem described by the general Poisson equation:

$$-\vec{\nabla} \cdot [\epsilon(\vec{r}) \nabla \vec{V}(\vec{r})] = 4\pi \rho_M(\vec{r}) \quad (2.23)$$

Simplified to

$$-\nabla^2 V(\vec{r}) = 4\pi \rho_M(\vec{r}) \quad (2.24)$$

$$-\epsilon \nabla^2 V(\vec{r}) = 0 \quad (2.25)$$

where C is the portion of space occupied by cavity, ϵ is dielectric function, V is the sum of electrostatic potential V_M generated by the charge distribution ρ_M and the reaction potential V_R generated by the polarization of the dielectric medium:

$$V(\vec{r}) = V_M(\vec{r}) + V_R(\vec{r}) \quad (2.26)$$

Polarizable Continuum Model (PCM) belongs to the class of polarizable continuum solvation models [23]. In PCM, the solute is embedded in a cavity defined by a set of spheres centered on atoms (sometimes only on heavy atoms), having radii defined by the van der Waals radius of the atoms multiplied by a predefined factor (usually 1.2). The cavity surface is then subdivided into small domains (called tesserae), where the polarization charges are placed. There are three different approaches to carry out PCM calculations. The original method is called Dielectric PCM (D-PCM), the second model is the Conductor-like PCM (C-PCM) [28] in which the surrounding medium is modeled as a conductor instead of a dielectric, and the third one is an implementation whereby the PCM equations are recast in an integral equation formalism (IEF-PCM). PCM Implicit solvation is utilized for our projects. All of the results of optimizations, transition states etc. derived from the calculations are models at 25 °C and 1 atm with B3LYP/6-31+G(d) methodology.

The activation Gibbs energy is calculated by modelling transition state geometries and reactants. Gibbs free energies of molecules are derived from the models and the activation free energies are calculated with the following formula;

$$\Delta G^{\ddagger} = G_{TS} - G_{diene} - G_{dienophile} \quad (2.27)$$

The reaction Gibbs energy is calculated by calculating the Gibbs Energies of the products and reactants of the respective Diels Alder's reactions. The difference between the Gibbs Energies of the products and the reactants is the reaction energy. The reaction energies are calculated with the following formula;

$$\Delta G_{rxn} = G_{product} - G_{diene} - G_{dienophile} \quad (2.28)$$

Because it is very important to analyze the ratio for endo and exo products in a reaction and The *endo:exo* selectivity is determined with a ratio formula as the following;

$$\frac{n_{exo}}{n_{endo}} = \frac{e^{-\frac{\Delta G^{\ddagger}_{exo}}{kT}}}{e^{-\frac{\Delta G^{\ddagger}_{endo}}{kT}}} \quad (2.29)$$

$$\%Exo = \left(\frac{n_{exo}}{n_{exo} + n_{endo}} \right) \times 100 \quad (2.30)$$

$$\%Endo = \left(\frac{n_{endo}}{n_{exo} + n_{endo}} \right) \times 100 \quad (2.31)$$

3. AIM OF THE STUDY

The main purpose of this research is to investigate the mechanism of two main Diels Alder Reactions, check their *exo/endo* selectivity in different media such as gaseous, ethanol, compare the computational results with the experimental findings and understand the origins of the stereoselectivity. The study is composed of two main parts. In the first part, the heterocyclic 1, 3 addition types of reactions are modeled in order to observe if there is any *exo/endo* selectivity and kinetically explain the mechanism of the reaction. The enantio selectivity control is widely observed, however the control of *exo/endo* selectivity has been found to be more difficult for Diels Alder's reactions. All the molecules and possible products and their transition states are modeled, in order to investigate the mechanism of α -pinenerole as dienophile with the diene 5-((*Z*)-benzylidene)-3-phenyl-2-(phenylimino) thiazolidine-4-thion. The second part focuses on the effect of the ionic liquid to the *exo/endo* selectivity. The Diels Alder Reactions taken from the study of Pawar et al are modeled in the absence and in the presence of a complex 1-ethyl-3-methylimidazolium chloride ([EMI⁺]) cation in ethanol. Their kinetic and thermodynamic characteristics are searched to understand the effect of the ionic liquid.

4. RESULTS AND DISCUSSION

4.1. Modeling the Diels Alder Reaction of thiones with α -pinene

In the study of Dogan *et al.*, 5-benzylidene-2-arylimino-3-aryl-thiazolidine-4-thiones were used as heterodienes in the inverse electron-demand hetero Diels Alder cycloadditions with norbornene as a dienophile at 25°C [29]. The reactions with norbornene were found to proceed with 100% *exo* selectivity as determined by NMR experiments. With these successful experimental results the origins of the stereoselectivity of the hetero Diels Alder cycloaddition was investigated by using quantum chemical computational models. Regarding the compatible results from the two studies, the same procedure has been applied by the same group for the reaction of α -pinene and 5-benzylidene-2-arylimino-3-aryl-thiazolidine-4-thione to understand the mechanism and in a search of the stereoselectivity along the path of the reaction [29]. The reaction of diene and dienophile as it is indicated in the Scheme 4.1 is held at 25°C and 1 atm. The synthesis of compound 3 and compound 4 shown in the Scheme 4.1 is desired to be achieved at first in dichloromethane and the Diels Alder reaction didn't occur. The same reaction has been run with the same conditions with xylene and acetic acid. The acetic acid solvation reaction is run for one hour with reflux and as a second trial with acetic acid overnight reaction is held while mixing. The reaction with xylene is refluxed for two days and the product formation was checked with thin layer chromatography. However, there was no cyclo adduct formed.

Figure 4.1 indicates the most stable product after the conformer search analysis and the most stable one is selected to be the one that is lowest in energy. The orientation of the phenyl rings that are connected to nitrogen are not on the plane; because they would cause steric hindrance. Regarding compound 3 indicated in the Scheme 4.1 the bulky group connected to the carbon atom number 5 is on the same plane with the main skeleton of the molecule; because the electron flow is facilitated easily and conjugation takes place on the planar geometry.

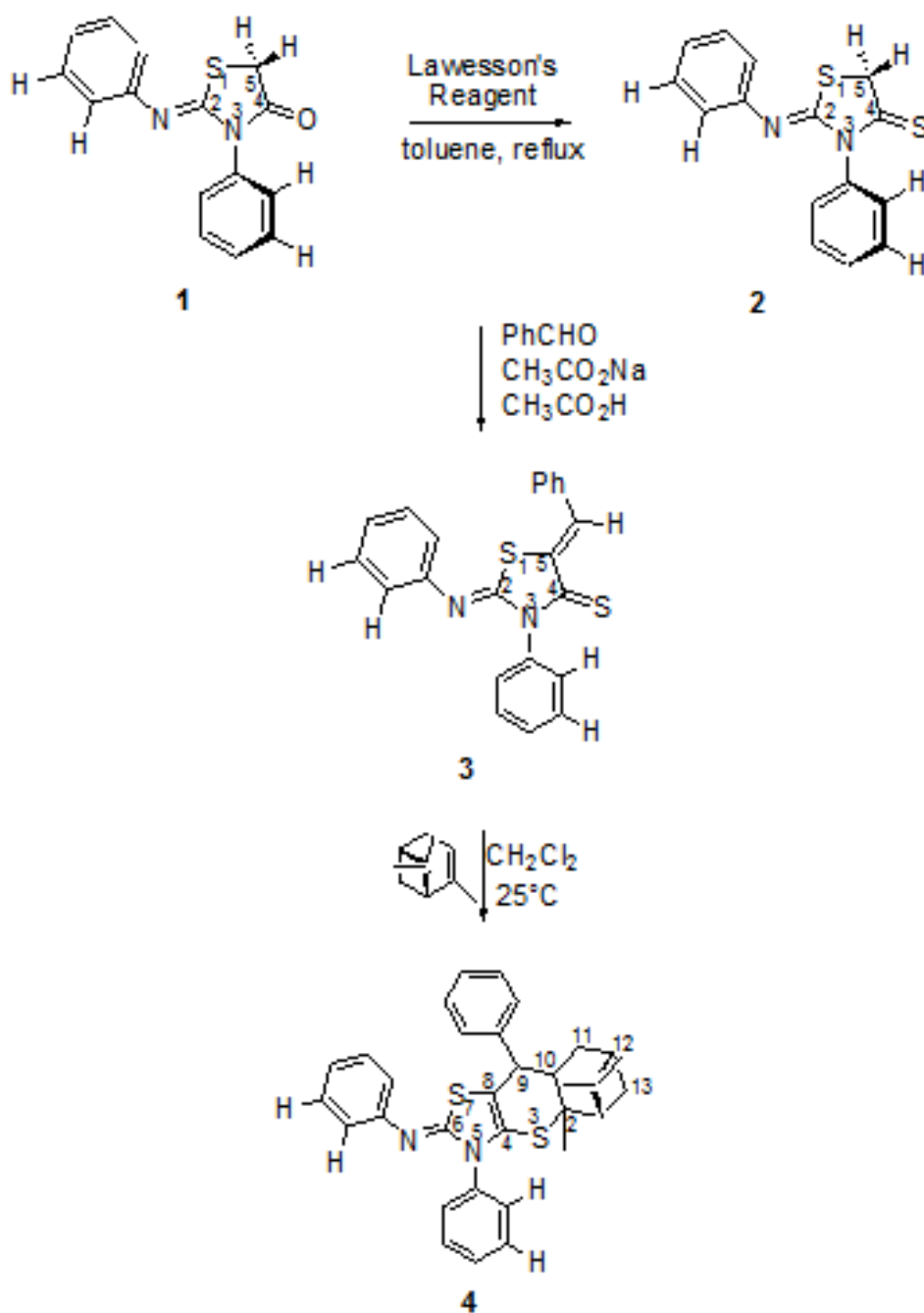


Figure 4.1. Representation of the Mechanism of the Reaction of (+) - α - Pinene with 5 - Benzylidene - 2 - Arylimino - 3 - Aryl - Thiazolidine - 4 - Thione.

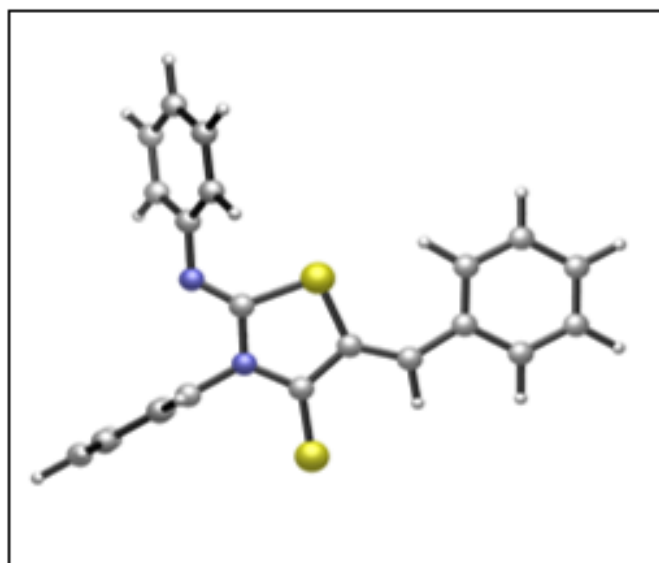


Figure 4.2. The Structure of the Diene, 5-((Z)-Benzylidene)-3-Phenyl-2-(Phenylimino)Thiazolidine-4-Thione.

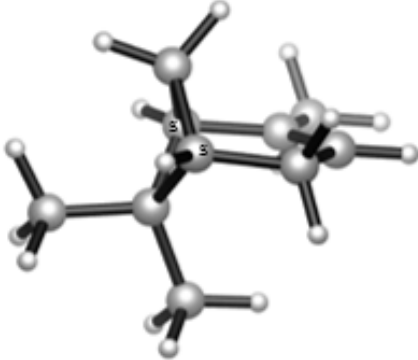
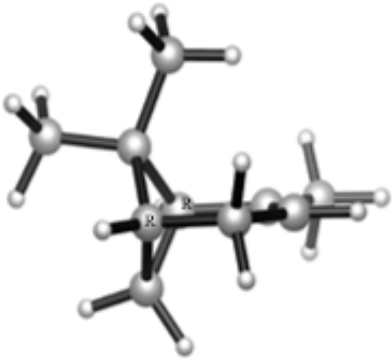
(+)- α -Pinene / SS	(-)- α -Pinene / RR
	
$G_{rel} = 0.00$ kcal/mol	$G_{rel} = 0.00$ kcal/mol
$G = -390.6701522$ Hartree	$G = -390.670152$ Hartree

Figure 4.3. The Structures of the two Stereoisomers of the Dienophile, Alpha Pinene with B3LYP/6-31+G(d).

According to the structure of α -pinene indicated in Figure 4.2, the enantiomers have the same electronic energy. Minus alpha pinene has been chosen in the reactions. The reaction between the diene, 5-benzylidene-2-arylimino-3-aryl-thiazolidine-4-thiones and dienophile, minus alpha pinene can take place in eight different ways. All

the combinations of diene and dienophile are considered according to the connectivity of the molecules. The combination is formed on the double bounded carbons of alpha pinene. The numbers are assigned to the respective carbons to follow up with bond formation mechanism. Referring to molecule (4) in Scheme 4.1., the methyl bounded carbon atom is labeled as C10 and the opposite double bond making carbon is labeled as C2 and sulphur atom on the dienophile is named as S3.

According to their connections the names of the products are given. For example, sulphur atom on the molecule (4), which is S3, is connected to C2. Therefore, the name of the product is labeled as S3C2-SRR. Moreover, the names include the information of the stereochemistry on the products. The three stereo centers that appear in the names referring to the chirality of the carbon number 9, 10 and 2, named as C9, C10, C2, of the molecule 4 that is demonstrated in the Scheme 4.1.

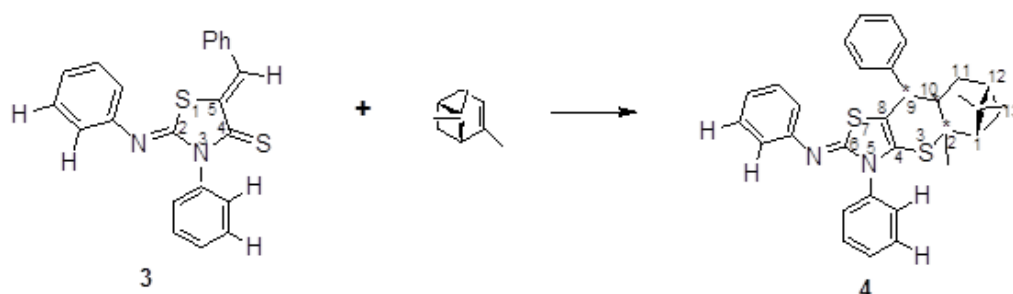


Figure 4.4. Diels Alder Reaction of 5 - ((Z) - Benzyldiene) - 3 - Phenyl - 2 - (Phenylimino) Thiazolidine - 4 - Thione with (-) α - Pinene.

The structures in Figure 4.3 and Figure 4.4 indicate the best conformers of the products found with B3LYP/6-31+G(d) in gaseous phase at 298.150 K and 1 atm. Two types of attacks are considered to make two connections between S3C10 and S3C2. Thermodynamically the most stable product is found to be S3C10-SRS; because the pendent phenyl rings are as far away from each other as possible from the bulky groups and the steric hindrance is minimized. The connectivity of S3 and C10 allows pinene to relax and find the best chair conformation. The most undesired combination of the respective Diels Alder reaction is S3C2-RSS; since the pinene bulky group causes

sterically limitations and increases the Gibbs free energy of the molecule.

All the relative Gibbs Energies are indicated in the Table 4.1. The *exo* and *endo* are almost equally stable. The reaction Gibbs Energies are found to be positive; indicating the reactions are endothermic. Moreover, the S3 with C10 connectivity is more favored than C2 connectivity; according to the thermodynamic data obtained.

In order to understand the mechanism and check the possibility of the synthesis of the respective products indicate in Figure 4.6; the transition are modelled with the same DFT methodology and activation energies are derived to evaluate the experimental results.

The same logic is utilized to name the transition states. The kinetic data is presented in Table 4.2.

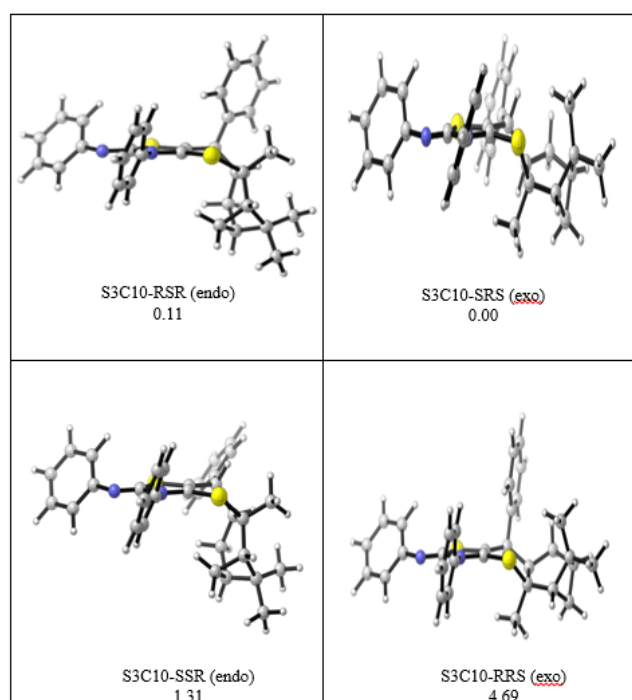


Figure 4.5. Products with S3C10 Connectivity Geometry. Relative Gibbs Free Energies are Given Below the Structures, in kcal/mol at 298.150 K and 1 atm.

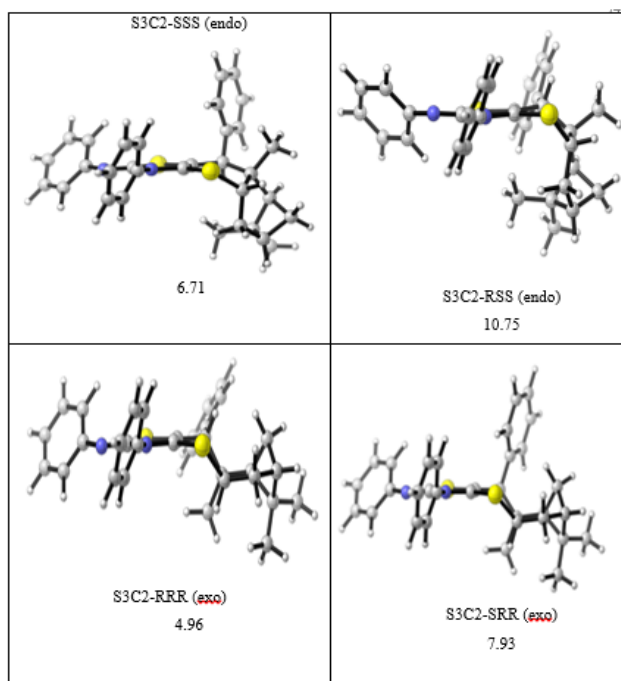


Figure 4.6. Products with S3C2 Connectivity Geometry. Relative Gibbs Free Energies are Given below the Structures, in kcal/mol at 298.150K and 1 atm.

Table 4.1. Thermodynamic Results of the Products Calculated with B3 LYP / 6 - 31 + G(d) at 298.150 K and 1 Atmin Gaseous Phase.

NAME OF PRODUCT	ΔG_{rxn} (kcal/mol)
S3C10-SRS (exo)	21.08
S3C10-RSR (endo)	21.18
S3C10-SSR (endo)	22.39
S3C10-RRS (exo)	25.76
S3C2-SSS (endo)	26.31
S3C2-RSS (endo)	26.79
S3C2-RRR (exo)	27.67
S3C2-SRR (exo)	33.39

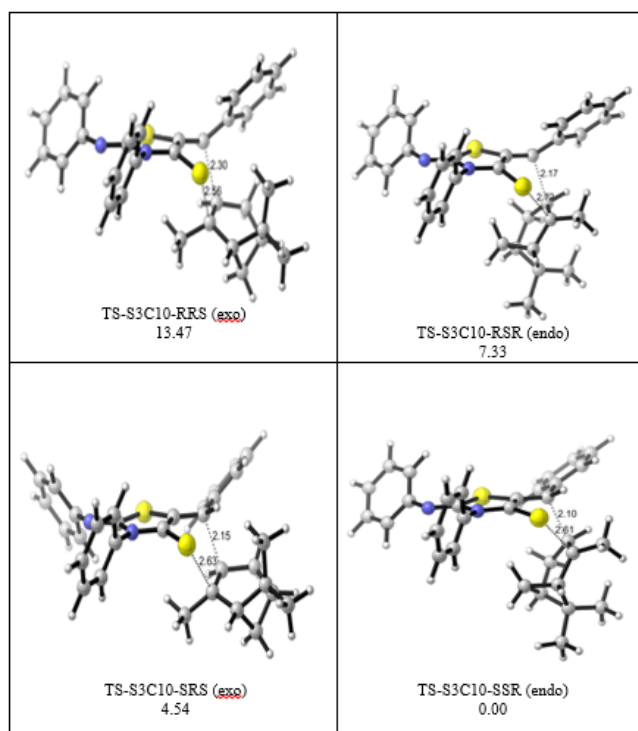


Figure 4.7. Transition States with S3C10 Connectivity Geometry. Relative Gibbs free Energies are given Below the Structures, in kcal/mol at 298.150 K and 1 atm.

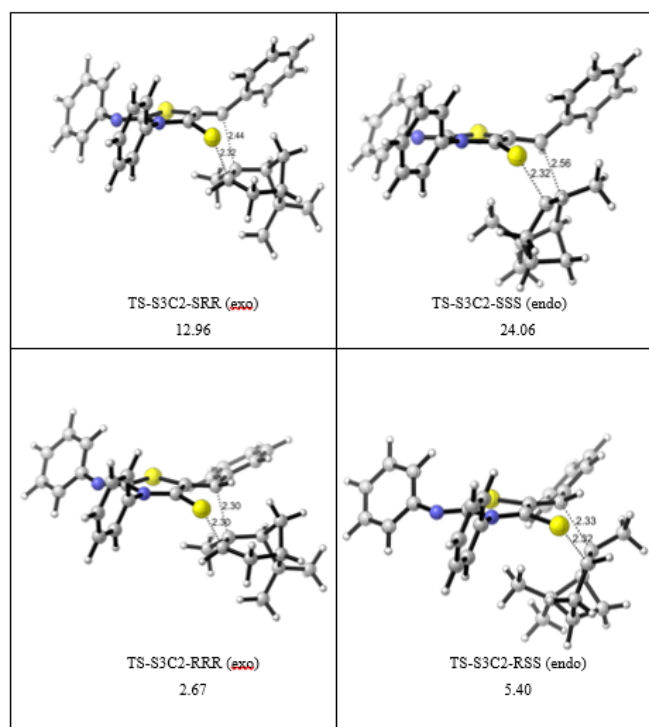


Figure 4.8. Transition States with S3C2 Connectivity Geometry. Relative Gibbs free Energies are Given Below the Structures, in kcal/mol at 298.150 K and 1 atm.

Table 4.2. Kinetic Data of the Transition State forms Calculated at 298.150 K and 1 atm in Gas.

NAME OF TS	ΔG^\ddagger (kcal/mol)
TS-S3C10-SSR (endo)	44.43
TS-S3C2-RRR (exo)	47.1
TS-S3C10-SRS (exo)	48.97
TS-S3C2-RSS (endo)	49.83
TS-S3C10-RSR (endo)	51.76
TS-S3C2-SRR (exo)	57.39
TS-S3C10-RRS (exo)	57.9
TS-S3C2-SSS (endo)	68.49

The eight transition states of the Diels Alder's reactions are modeled with the same methodology in order to understand why the experiments don't result with the synthesis of the modeled products. The activation Gibbs free energies are found to be relatively high for the Diels Alder's reactions to be achieved with the conditions mentioned in the experimental part. Moreover, the models of the transition states prove also that endo selectivity would be preferred if the reactions were performed; because the ΔG^\ddagger of the endo transition states are relatively lower than the *exo* transition state according to the calculations. The fastest reaction is found to be with the endo transition state named as TS-S3C10-SSR according to the activation energy of reactions calculated and indicated in Table 4.2. The Gibbs free relative energy of the best structure of endo transition state is found to be 2.67 kcal/mol lower than the best structure of *exo* transition state. Being the most stable transition state, TS-S3C10-SSR (endo) has both lowest relative energy and activation energy. This property is handled because phenyl group on C10 doesn't come on the same side with methyl group on the alpha pinene. This orientation of the bulky groups eliminates the steric hindrance constraints. Moreover, S3 has relatively more flexible space to interact with the targeted atom on pinene; since the methyl group is located upper wards. The least stable transition state is TS-S3C2-SSS (endo). The reason why it is not preferred

thermodynamically is the steric hindrance between the phenyl ring on C10 and methyl group on pinene. These bulky groups don't allow diene and dienophile to come close to interact.

4.2. Modeling the Diels Alder Reactions of Cyclopentadiene with Methacrylate Derivatives

Regarding the importance of the effect of the ionic liquid on the cycloaddition of cyclopentadiene with methacrylate derivatives, the three main reactions are modeled without ionic liquid in order to be able to compare the effect of the ionic liquid and understand the mechanism of the Diels Alder reactions taken from the Pawar *et al.*, in silico.

4.2.1. Modeling the Diels Alder Reactions of Cyclopentadiene with Methacrylate Derivatives in the Absence of Ionic Liquids

The thermodynamic and kinetic results of all the reactants, possible products and the transition states are given in Table 4.3 and Table 4.4. The nomenclature of the modelled molecules is given according to the numbers given in the Pawar Kumar's study as 3 when there is no functional group on the C4 in Figure 4.8. If methyl group is not on the C4; but on the C3 position and it is named as 5 if it has a skeleton indicated in Figure 4.8. It is named endo if the $-\text{COOCH}_3$ group is on the inverse direction with the bridging carbon on the position 5 on the Figure 4.8. If the $-\text{COOCH}_3$ group is on the same direction with the bridging carbon on the position 5 on the Figure 4.8 then the molecule is named as *exo*.

The molecule is named according the stereo centers indicated in the Figure 4.8. The position 4 is a chiral center only for molecule 5 from the Pawar et al's study [15]. These three diene molecules are modeled as anti and syn orientation. The products and the transition states of the three reactions are modeled regarding all the combination of connectivity and all the possible stereogenic centers are modeled. The enantiomeric structures are found to be energetically the same. Therefore, we derive four products

of 3 and 4 and eight products of 5 molecules. The kinetic and thermodynamic data is indicated in the Table 4.3.

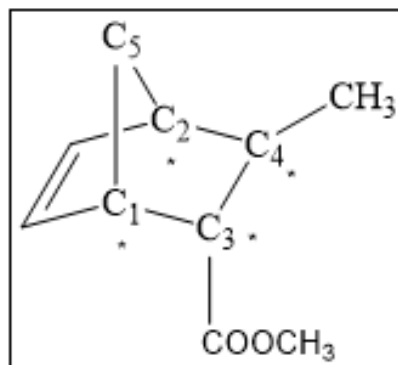


Figure 4.9. The Positions of the Stereo Centers of the Molecules.

Table 4.3. The Thermodynamic and Kinetic Results of the Molecules via B3 LYP / 6-31 + G(d) at 298.150K and 1 atm. Gibbs free Energies are given in (kcal/mol).

	Name of the compound	GibbsFreeEnergy (Hartree)	G_{rel}	ΔG^\ddagger	ΔG_{rxn}
	cyclopentadiene	-194.046.699			
REACTANTS	2a-syn	-306.424.027	0.00		
	2a-anti	-306.423.412	0.39		
	2b-syn	-345.716.611	0.00		
	2b-anti	-345.716.628	0.01		
	2c-syn	-345.720.567	0.00		
	2c-anti	-345.721.313	0.47		
TRANSITION STATES	TS-3-endo-SSS / RRR	-500.418.996		32.46	
	TS-3-exo-SSR / RRS	-500.417.844		33.18	
	TS-4-endo-SSS / RRR	-539.704.827		36.7	
	TS-4-exo-SSR / RRS	-539.705.799		36.09	
	TS-5-endo-SRSR / SRRS	-539.707.009		37.81	
	TS-5-exo-SRRS / SRSR	-539.706.705		38.00	
PRODUCTS	3-endo-SSS / RRR	-500.465.941	0		3.00
	3-exo-SSR / RRS	-500.465.477	0.29		3.29
	4-endo-SSS / RRR	-539.750.951	0.00		7.77
	4-exo-RRS / SSR	-539.750.200	0.47		8.24
	5-endo-SRSR / SRRS	-539.754.558	0.08		7.97
	5-exo-SRRS / SRSR	-539.754.692	0.00		7.89
	5-endo-SRSS / SRRR	-539.750.212	2.81		10.70
	5-exo-SRSR / SRRS	-539.751.159	2.21		10.11

Thermodynamically calculations indicate that all the methacrylate molecules

tend to form syn products. The kinetic results of the calculation indicate the *endo* product is favorable for the molecule **3** and for **5** and *exo* product is preferred for **4** kinetically.

Table 4.4. The *exo-endo* Ratios Calculated in the Absence of Ionic Liquid in Ethanol.

Name of Transition State	Exo-Endo Ratio	Endo Percentage	Experimental Pawar-Kumar[15]
3-endo-SSS	0.30	77	84
3-exo-SSR		23	16
4-endo-SSS	2.80	26	35
4-exo-SSR		74	65
5-endo-RRSS	0.72	58	62
5-exo-RSSR		42	38

Table 4.4 indicates that 77% of the products of molecule **3** formed is *endo*; 74% of the products of **4** is *exo* and molecule **5** prefers to produce *endo* with 58% of its products. All of these results are consistent with the findings of experimental findings mentioned in the literature [15].

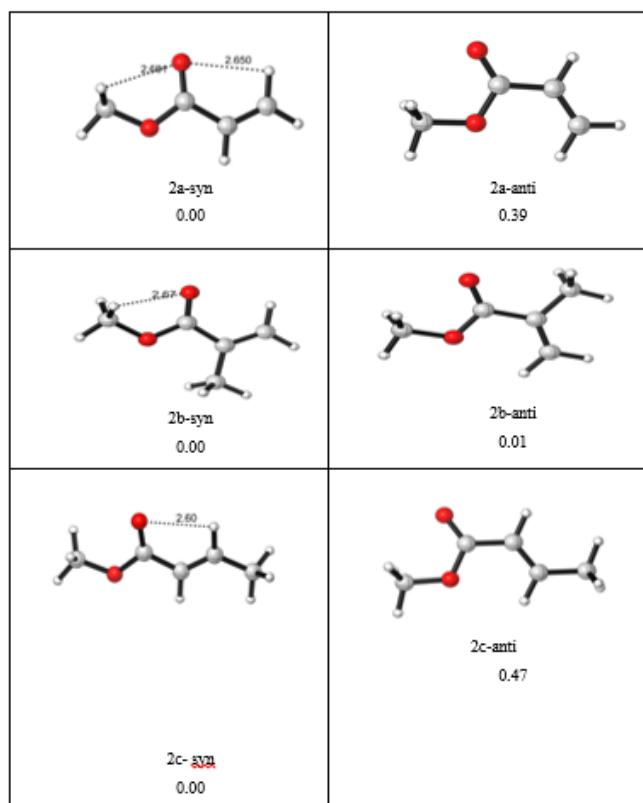


Figure 4.10. The Positions of the Stereo Centers of the Molecules Relative Gibbs Free energy of the Conformers of the Dienophile Modeled in Ethanol.

According to Figure 4.9 the most stable molecules of dienophiles are the syn reactants; because the hydrogen and oxygen are in H-bonded to each other and the conjugation between carbonyl and double bond of acrylate is feasible.

For molecule **4** *exo* selectivity while for molecule **3** and **5** *endo* selectivity is dominant. The fastest reaction is found to form 3-endo-SSS / SSR according to the kinetic data derived, that is having the lowest activation energy 32.46 kcal/mol like it is shown in the Figure 4.11.

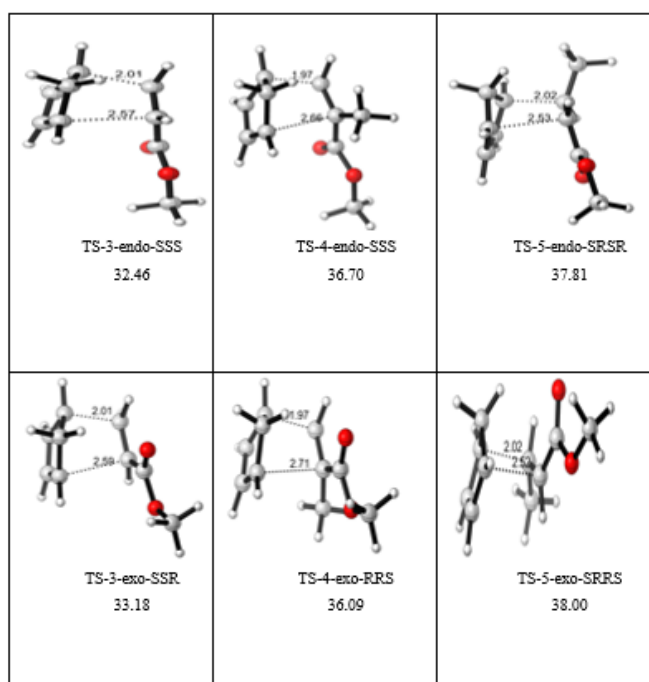


Figure 4.11. Activation Energies of the Transition State Structures Modeled in Ethanol.

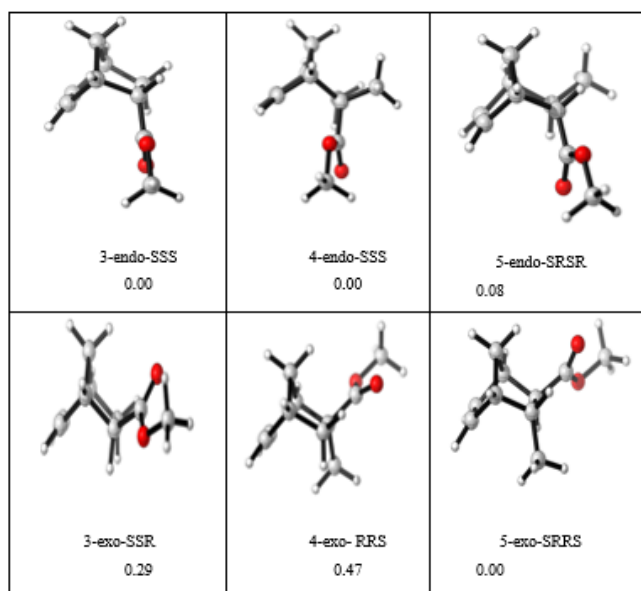


Figure 4.12. Relative Gibbs Free Energies of Products Modeled in Ethanol.

According to Figure 4.12, the most stable products are *endo* character for **3** and **4**. The product **5-endo-SRSR** is the hardest to form due to the steric hindrance on the methyl and methacrylate functional groups.

4.2.2. Modeling the Diels Alder Reactions of Cyclopentadiene with Methacrylate Derivatives in the Presence of Ionic Liquids

Endo selectivity is observed for two molecules and *exo* selectivity in one reaction in the modeling the reactions of Pawar's study in the absence of ionic liquid, which is also found on the experimental results. This selectivity is tested if there is any change in the trend of the selectivity with the addition of ionic liquid. The ionic liquid is chosen to be 1-ethyl-3-methylimidazolium cation. The interaction of hydrogens on the ring is targeted to interact with the carbonyl of methacrylate and enhance the rate of the cycloaddition reactions. The partial charges on the dienophiles are calculated as it is indicated in the Figure 4.1 and Table 4.5. The atom's partial charges are utilized to understand the reactivity of where the ionic liquid should be expected.

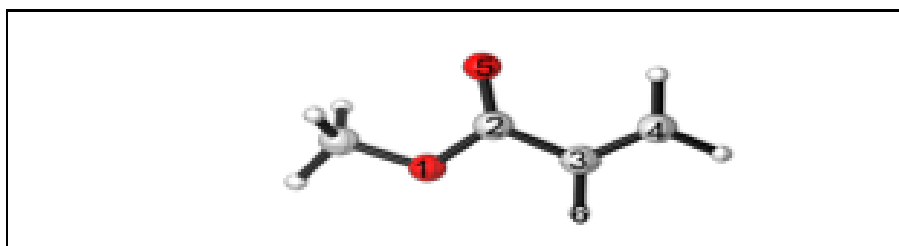


Figure 4.13. Numbering Used in Methyl Metacrylate Derivatives.

Table 4.5. NPA charges on the reactant with B3LYP/6-31+G(d) in ethanol.

Reactant	O1	C2	C3	C4	O5	C6
2a-syn	-0.551	0.774	-0.342	-0.343	-0.614	0.251
2a-anti	-0.56	0.773	-0.333	-0.355	-0.604	0.256
2b-syn	-0.551	0.774	-0.342	-0.343	-0.614	-0.706
2b-anti	-0.558	0.791	-0.135	-0.362	-0.609	-0.704
2c-syn	-0.554	0.778	-0.356	-0.122	-0.623	0.246
2c-anti	-0.564	0.777	-0.347	-0.132	-0.611	0.25
2a-IL	-0.525	0.805	-0.339	-0.332	-0.687	0.269
2b-IL	-0.531	0.821	-0.137	-0.344	-0.687	-0.711
2c-IL	-0.554	0.778	-0.356	-0.122	-0.623	0.246

It is found that the most attractive oxygen on the methacrylate derivatives is O5 as it is indicated in the Table 4.5. The thermodynamic data and the kinetic results for the models with ionic liquid are given on the Table 4.6. The ‘-IL’ ending means the molecule is modeled with the ionic molecule. The syn dienophiles are chosen and the modeled transition states and product from the models in the presence of ionic liquid.

Table 4.6. The Thermodynamic and Kinetic Results of the Molecules at 298.150 K and 1 atm. Gibbs Free Energies are given in kcal/mol.

Ionic Liquid-Ethanol	Name of the Compound	Gibbs Free Energy (Hartree)	G_{rel}	ΔG^\ddagger	ΔG_{rxn}
REACTANTS	cyclopentadiene	-194.046.699			
	2a-IL	-650.904.979			
	2b-IL	-690.196.338			
	2c-IL	-690.201.249			
TRANSITION STATES	TS-3-endo-SSS-IL	-844.898.826		33.17	
	TS-3-exo-RRS-IL	-844.897.306		34.12	
	TS-4-endo-RRR-IL	-884.184.315		36.85	
	TS-4-exo-RRS-IL	-884.185.203		36.29	
	TS-5-endo-SRSR-IL	-884.186.179		38.76	
	TS-5-exo-SRRS-IL	-884.184.640		39.72	
PRODUCTS	3-endo-SSS-IL	-844.943.473	0.33		5.15
	3-exo-RRS-IL	-844.943.995	0.00		4.82
	4-endo-RRR-IL	-884.229.127	0.00		8.73
	4-exo-RRS-IL	-884.228.385	0.47		9.19
	5-endo-SRSR-IL	-884.231.660	1.02		10.22
	5-exo-SRRS-IL	-884.233.292	0.00		9.20

According to the results of the calculations in Table 4.6, molecule **3** has the *endo* ratio increased; whereas molecule **4** has higher *exo* product yield. Furthermore, Table 4.6 indicates that the ionic liquid effect neither made a dramatic effect on the kinetics of the reaction nor reinforced the tendency of the *endo* selectivity.

According to Table 4.7 *endo* selectivity in the ionic liquid medium is found 83% out of the all products modeled. The charge on the ionic liquid is distributed differently on the cationic structure of the 1-Ethyl-3-methylimidazolium without chloride.

The hydrogen number 1 in the Figure 4.14 interacts with the carbonyl of the respective reactants. This hydrogen was expected to be the most partially negative

Table 4.7. The exo-endo Ratios Calculated in the Presence of Ionic Liquid in Ethanol.

Name of Compound	Exo-Endo Ratio	Endo Percent
3-endo-SSS-IL	0.2	83
3-exo-RRS-IL		17
4-endo-RRR-IL	0.39	28
4-exo-RRS-IL		72
5-endo-SRSR-IL	0.2	84
5-exo-SRRS-IL		16

one. However, it wasn't found to be the most electron dense according NPA population analysis. Therefore, the ionic liquid is not observed to have the exactly targeted catalyst function; although the models of the transition state and the distance of the ionic liquid and the reactants are set properly.

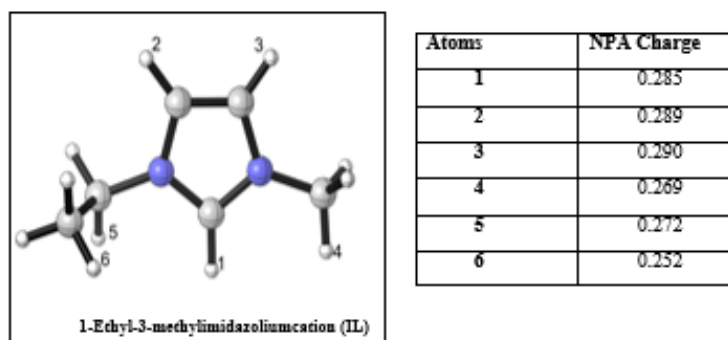


Figure 4.14. 1-Ethyl-3-Methylimidazolium Cation with its NPA Charges on the Hydrogen Atoms.

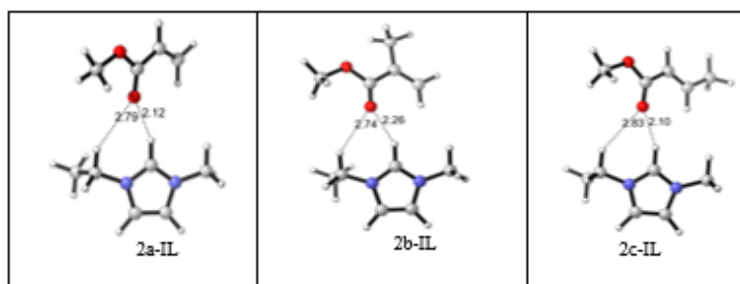


Figure 4.15. Reactants with Ionic Liquid Modeled with B3LYP/6-31+G(d) in Ethanol.

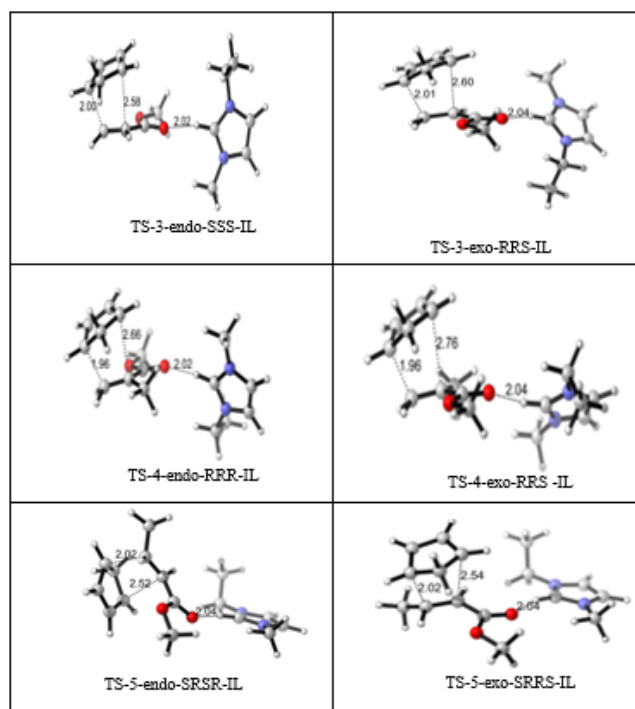


Figure 4.16. Transition State Structures Modeled with B3LYP/6-31+G(d) in Ethanol.

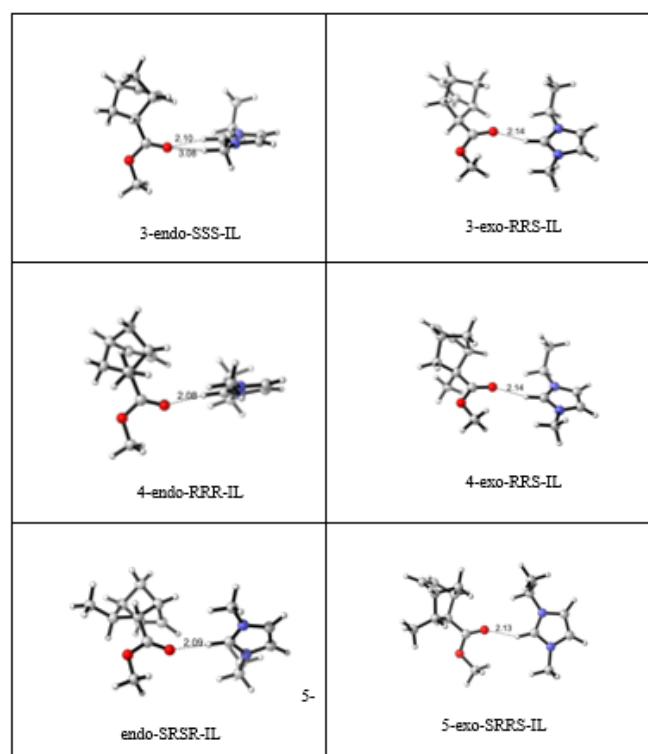


Figure 4.17. Product Structures Modeled with B3LYP/6-31+G(d) in Ethanol.

The interaction of the respective ionic liquid is found to be with the dienophiles. The carbonyl oxygen and the hydrogen on carbon are targeted to be the most stabilizing interactions (Figure 4.15).

The fastest reaction is achieved with TS-3-endo-SSS-IL having the lowest activation Gibbs free energy as 33.17 kcal/mol.

5. CONCLUSION

The models of the eight Diels Alder's reactions of alpha pinene are compared with the experimental findings. Not being able to have the desired reactions experimentally in different solutions is explained as the result of having very high activation barriers calculated in gaseous phase at 298.150 K and 1 atm.

In the second part the reactions are modeled in ethanol with B3LYP/6-31+G(d) methodology[30] and the exo selectivity is found to be consistent with the experimental results mentioned in Kumar *et al.*'s work in the absence of ionic liquid.

The ionic liquid effect is not found to be dramatically shifting the tendency of the selectivity; because the anion of the respective salt is not included; that is all the reactions are modeled with the cation.

6. FUTURE WORK

As a future work, molecules resembling norbornene can be modeled and their Diels Alder's reactions with thiazolidine-4-thione derivatives. Another investigation for the second part of the dissertation with the same ionic liquid can be performed *in silico* in order to see the interaction of the other hydrogens on the structure of the ionic liquid. For the second part of the study the cation of the ionic liquid has utilized. The investigation can be performed with the addition of chloride anion. *In silico* studies can be performed with other types of ionic liquids.

REFERENCES

1. Kobayashi, S. and K.A. Jørgensen, "Cycloaddition Reactions in Organic Synthesis", *Wiley-WCH*, Germany, 2002.
2. Dereli, B., M.S. Thesis, "Modeling the Isomerization of Lactones and the Role of Catalysts in Hetero-Diels-Alder reactions", 2013.
3. Houk, K.N., Y.T. Lin and F.K. Brown, "Evidence for the Concerted Mechanism of the Diels-Alder Reaction of Butadiene with Ethylene", *Journal of the American Chemical Society*, Vol. 108, pp. 554-556, 1986.
4. Andrushko, V., N. Andrushko, "Stereoselective Synthesis of Drugs and Natural Products", *John Wiley & Sons*, Vol.1, pp. 1-1683, 2013.
5. Wang, H. and K. N. Houk, "Torsional Control of Stereoselectivities in Electrophilic Additions and Cycloadditions to Alkenes", *chemical-Science*, Vol. 5, pp. 462-470, 2014.
6. AgopcanCinar, S. and V. Aviyente, "Origins of exo-Stereoselectivity of Norbornene in Hetero Diels-Alder Reactions", *Organic & Biomolecular Chemistry Journal*, 2013.
7. Diels, O., K. Alder, "Synthesen in der Hydroaromatischen Reihe, I", *Justus Liebig's Annalen der Chemie*, Vol. 460, pp. 98-122, 1928.
8. Sahu, D., M.K. Kesharwani, G. Ganguly, "Origin of Reversal of Stereoselectivity for [4+2] Cycloaddition Reaction Between Cyclopentadiene and Methyl Methacrylate in the Presence of the Chloroaluminate Ionic Liquid (1-ethyl-3-Methyl-Imidazolium Chloride): in Silico Studies", *Canadian Journal of Chemistry*, Vol. 92, pp. 862-867, 2014.

9. Acevedo, O., "Determination of Local Effects for Chloroaluminate Ionic Liquids on Diels-Alder Reactions", *Journal of Molecular Graphics and Modelling*, Vol. 28, pp. 95-101, 2009.
10. Swapnil A.D., M.N. Varma, D. Z. Shende, K. Y. Chang, K. L. Wasewar, "Synthesis, Characterization and Application of 1-Butyl-3 Methylimidazolium Chloride as Green Material for Extractive Desulfurization of Liquid Fuel" *The Scientific World Journal*, Vol. 2013, pp. 1-9, 2013.
11. M. Koel, "Ionic Liquids in Chemical Analysis" *Chemical Rubber Company Press*, 2008.
12. R.P. Swatloski, J.D. Holbrey and R.D. Rogers "Ionic liquids are not always green: hydrolysis of 1-butyl-3-methylimidazolium hexafluorophosphate", *Green Chemicals*, Vol. 5 (4), pp.361-363, 2003.
13. Dupont, J., Consorti, C., Suarez, P., de Souza, R. "Preparation of 1-Butyl-3-Methyl Imidazolium-Based Room Temperature Ionic Liquids", *Organic Syntheses*, Vol. 10, pp. 184, 2004.
14. J. B. Binder, T.R. Ronald, "Fermentable Sugars by Chemical Hydrolysis of Biomass", *Proceedings of the National Academy of Sciences of the United States America*, Vol. 107-10, pp. 4516-4521, 2010.
15. Kumar A. and S.S. Pawar, "Converting exo-Selective Diels-Alder Reaction to endo-Selective in Chloroaluminate Ionic Liquids", *Journal of Organic Chemistry*, Vol. 69, pp. 1419-1420, 2004.
16. Becke, A.D., "Density-Functional Exchange Energy Approximation with Correct Asymptotic Behavior", *Physical Review A*, Vol. 38, pp. 3098-3103, 1988.
17. Becke A. D., "A New Mixing of Hartree-Fock and Local Density Functional Theories", *Journal of Chemical Physics*, Vol. 38, pp. 1372-1377, 1993.

18. Parr, R. G. and W. Yang, "Density Functional Theory of Atoms and Molecules", *Oxford University Press*, New York, 1989.
19. Handy, N.C., "Density Functional Theory", *Springer-Verlag*, Vol. 2, pp. 91-123, 1994.
20. Leach, A.R., "Molecular Modelling Principles and Applications", *Prentice Hall*, England, 2001.
21. Lee, C., W. Yang and R. G. Parr, "Development of Colle-Salvatti Correlation Energy Formula into a Functional of the Electron Density", *Physical Review B: Condensed Matter and Materials Physics*, Vol. 37, pp. 785-789, 1988.
22. Becke, A. D., "Density Functional Thermochemistry. III. the Role of Exact Exchange", *The Journal of Chemical Physics*, Vol. 98, pp. 5648-5652, 1993.
23. Barone, V., M. Cossi and J. Tomasi, "Geometry Optimization of Molecular Structures in Solution by the Polarizable Continuum Model", *Journal of Computational Chemistry*, Vol.19, pp. 404-417, 1998.
24. Pauling, L. J., "The Nature of the Chemical Bond. IV. The Energy of Single Bonds and the Relative Electronegativity of Atoms", *Journal of the American Chemical Society*, Vol. 54, pp. 3570-3582, 1932.
25. Tapia, O. and J. Bertrán, "Solvent Effects and Chemical Reactivity", *Kluwer Academic Publishers*, 1996.
26. Cramer, C. J. and D. G. Truhlar, "Implicit Solvation Models: Equilibria, Structure, Spectra, and Dynamics", *Chemical Reviews*, Vol. 99, pp. 2162-220, 1999.
27. Tomasi, J., B. Mennucci and R. Cammi, "Quantum Mechanical Continuum Solvation Models", *Chemical Reviews*, Vol. 105, pp. 2999-3093, 2005.
28. Barone, V. and M. Cossi, "Quantum Calculation of Molecular Energies and Energy

Gradients in Solution by a Conductor Solvent Model”, *The Journal of Physical Chemistry A.*, Vol. 102, pp. 1995-2001, 1998.

29. Erol, S. and I. Dogan, “exo-Selective Inverse-Electron-Demand Hetero Diels-Alder Reactions of Norbornene with 5-Benzylidene-2-Arylimino-3-Aryl-Thiazolidine-4-Thiones at Room Temperature”, *Tetrahedron*, Vol. 69, pp. 1337-1344, 2013.
30. Gaussian 09, Revision A.1, M. J. Frisch, G. W. Trucks, H. B. Schlegel, G. E. Scuseria, M. A. Robb, J. R. Cheeseman, G. Scalmani, V. Barone, B. Mennucci, G. A. Petersson, H. Nakatsuji, M. Caricato, X. Li, H. P. Hratchian, A. F. Izmaylov, J. Bloino, G. Zheng, J. L. Sonnenberg, M. Hada, M. Ehara, K. Toyota, R. Fukuda, J. Hasegawa, M. Ishida, T. Nakajima, Y. Honda, O. Kitao, H. Nakai, T. Vreven, J. A. Montgomery, Jr., J. E. Peralta, F. Ogliaro, M. Bearpark, J. J. Heyd, E. Brothers, K. N. Kudin, V. N. Staroverov, R. Kobayashi, J. Normand, K. Raghavachari, A. Rendell, J. C. Burant, S. S. Iyengar, J. Tomasi, M. Cossi, N. Rega, J. M. Millam, M. Klene, J. E. Knox, J. B. Cross, V. Bakken, C. Adamo, J. Jaramillo, R. Gomperts, R. E. Stratmann, O. Yazyev, A. J. Austin, R. Cammi, C. Pomelli, J. W. Ochterski, R. L. Martin, K. Morokuma, V. G. Zakrzewski, G. A. Voth, P. Salvador, J. J. Dannenberg, S. Dapprich, A. D. Daniels, Ö. Farkas, J. B. Foresman, J. V. Ortiz, J. Cioslowski, and D. J. Fox, “Gaussian, Inc.”, *Wallingford CT*, Vol. 3, pp. 2001-2004, 2009.